Soft Matter

COMMUNICATION

View Article Online
View Journal

Bioadhesive giant vesicles for monitoring hydroperoxidation in lipid membranes†

P. H. B. Aoki,[abc] A. P. Schroder,*[a] C. J. L. Constantino[b] and C. M. Marques[a]

Cite this: DOI: 10.1039/c5sm01019e

Received 28th April 2015,
Accepted 3rd June 2015

DOI: 10.1039/c5sm01019e

www.rsc.org/softmatter

Osmotic stresses, protein insertion or lipid oxidation lead to area increase of self-assembled lipid membranes. However, methods to measure membrane expansion are scarce. Challenged by recent progress on the control of phospholipid hydroperoxidation, we introduce a method to quantitatively evaluate membrane area increase based on the bio-adhesion of Giant Unilamellar Vesicles.

Lipid photo-oxidation is a natural outcome of life under oxygen and essential for Photodynamic Therapy of cancer tissues.[1,2] Hydroperoxidation, a prominent pathway for lipid oxidation, results in the insertion of the organic hydroperoxide group OOH at the unsaturated bond site.[3–5] At the molecular level, the increased hydrophilicity of the lipid chains carrying the OOH groups changes the statistical distribution of chain conformations and leads noticeably to the increase of the area per lipid. Degree of membrane oxidation, and the associated changes in membrane properties such as membrane shape, elasticity or permeability[6–8] can thus be monitored by a measure of membrane area increase.

Previous methods to monitor membrane area changes following oxidation relied on the application of micropipette suction techniques or external electric fields to Giant Unilamellar Vesicles (GUVs).[7,8] While micropipette suction recently provided the first values for oxidized lipid area expansions, its implementation is not straightforward. In particular, pipettes have to be pulled and forged, coupled to a hydrostatic device before being monitored in the microscope objective vicinity through a high precision, *i.e.* micrometer range, *XYZ* manipulation device. Measuring membrane deformation by electric fields is more straightforward and contactless, requiring a rather common technology.[9] However, the method requires ionic contrast between the internal and external GUVs solutions which the membranes might not be able to maintain as for instance in the case of transient pore formation, a phenomenon already observed during lipid oxidation.[6]

In the quest for a method to determine membrane area increase that is (i) fast and easy, (ii) effectively reliable even in the case of increased membrane permeability (due to transient pore formation or any other mechanism), we developed a bio-mimetic approach based on the geometrical changes that follow oxidation of GUVs strongly adhered on a substrate. The method can be easily implemented by simply (i) preparing GUVs from a mixture of the desired lipids with a small fraction (2% or less) of commercially available biotinylated lipids, (ii) let the giant vesicles sediment onto streptavidinated substrates also commercially available or prepared by well documented methods,[10,11] (iii) measure the size of the vesicle adhesion patch by reflection interference contrast microscopy (RICM),[12] a technique available for standard optical microscopes, that can furthermore be implemented in a lighter version than the one commonly described in the literature, as explained into the ESI† section. As demonstrated below, one advantage of the technique stems from the easy and straightforward monitoring that no loss of internal liquid occurs during the experiment. Indeed, any membrane pore formation leads in the present geometry to a dramatic, easily detected decrease of the GUV volume, due to the strong adhesion conditions.

In this communication we show the feasibility and advantages of the method by measuring the area increase of POPC and DOPC GUVs oxidized in a solution of the photosensitizer erythrosin. Under irradiation at 547 nm, excited states of erythrosin can transfer energy to O_2, the molecular oxygen of the solution, thus generating singlet oxygen $^1O_2$.[13] This reactive oxygen species diffuses in the solution over an average length of 100 nm before decaying. Reactions of singlet oxygen with the unsaturated bonds of the lipid chains generate hydroperoxide groups that further induce an increase of area per lipid, due to the molecular-scale modification of the carbon chain hydrophilic–hydrophobic balance. In the present study we measure a specific area increase per lipid of *circa* 14% for POPC and 18% for DOPC, *i.e.* values that are in complete agreement with the ones previously

[a] *Institut Charles Sadron, Université de Strasbourg, CNRS UP 22, F-67034 Strasbourg Cedex 2, France. E-mail: andre.schroder@ics-cnrs.unistra.fr*
[b] *Faculdade de Ciências e Tecnologia, UNESP Universidade Estadual Paulista, Presidente Prudente, SP, 19060-900, Brazil*
[c] *São Carlos Institute of Physics, University of São Paulo, CP 369, 13560-970 São Carlos, SP, Brazil*

† Electronic supplementary information (ESI) available. See DOI: 10.1039/c5sm01019e

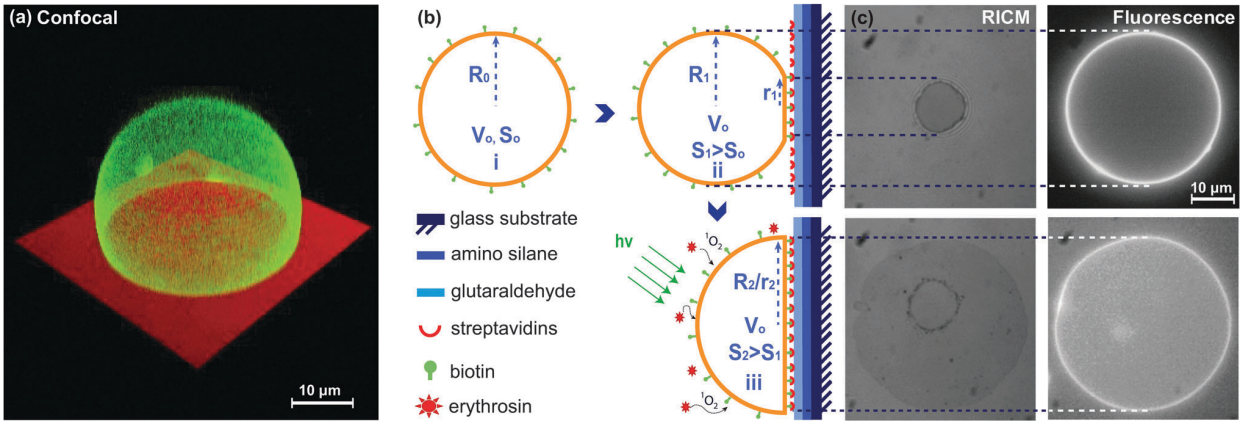

Fig. 1 (a) Three-dimensional reconstitution of a typical adhered GUV, obtained from confocal microscopy. (b) Schematic representation of streptavidin molecularly-designed surfaces, biotinylated GUVs and the three-step sequence of the bio-adhesion method; (i) free standing GUV as introduced in the observation cell; (ii) non oxidized adhered GUV as obtained after sedimentation of the free standing GUVs; (iii) oxidized GUV. GUVs and bio-molecule sizes do not fit true scale. (c) Biotinylated DOPC GUV adhered onto a streptavidin-covered surface, in a buffer containing 25 μM of erythrosin, as recorded with fluorescence microscopy and RICM, before (above) and after (below) irradiation.

obtained by us on the same systems, using the micropipette aspiration technique.[8]

Our method relies on a two-step procedure. First, we prepare a substrate with adhered vesicles in the absence of any oxidation. Then, we oxidize the adhered vesicles and measure the associated membrane area increase. Fig. 1a shows a three-dimensional reconstitution of a typical adhered GUV, obtained from confocal microscopy: the adhered vesicle has a shape composed of a circular adhered patch and a spherical section of radii r and R respectively (see the ESI† section for the justification of the GUV shape as a result of strong adhesion). The original GUVs, prepared in the bulk with radius R_0, volume V_0 and surface S_0 are driven down to the bottom of the observation cell, due to gravity forces, where they adhere in less than 10 seconds due to their strong affinity for the substrate surface, into a final shape with radii r_1 and R_1 – see Schemes I and II in Fig. 1b. Fig. 1c shows also how r_1 and R_1 can be determined by RICM and fluorescence microscopy respectively. As explained in ESI,† adhesion at that stage takes place at constant volume V_0 due to the sugar content of the solution; also, no vesicle bursting occurs under our strong adhesion conditions. This results in the increase of the apparent area of the vesicle from S_0 to S_1 corresponding to the unfolding of the original excess membrane, systematically present in GUVs obtained from electroformation, usually detected (in absence of any adhesion) by the presence of the thermally activated membrane fluctuations. Concomitantly to the membrane adhesion, the membrane tension increases up to a value where the Young's law for vesicle adhesion is obeyed.[14–16] At this point tension and adhesion forces are balanced.

For a transformation in vesicle shape at constant volume V_0, there is a one-to-one relation between the patch radius r and the membrane area S, as quantitatively explained in the ESI† and plotted in Fig. 2a, where a theoretical projection of the relative surface area expansion $(S/S_0 - 1)$ as a function of the reduced radius (r/R_0) of the adhered patch is shown. For typical experimental conditions this first step of adhesion results in a

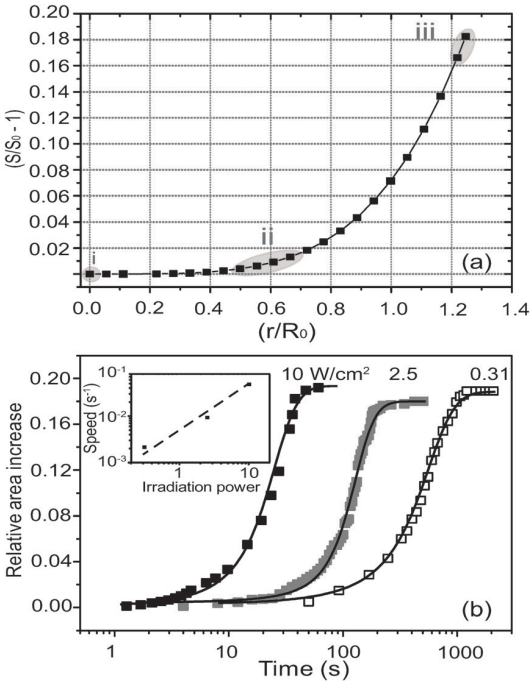

Fig. 2 (a) Theoretical projection of the relative surface area expansion $(S/S_0 - 1)$ as a function of the reduced radius of the adhered patch (r/R_0), calculated from equations available at ESI.† (b) Evolution with time of relative surface area increase $(S_2/S_1 - 1)$, considering different irradiation powers (10, 2.5 and 0.31 W cm^{-2}), for three DOPC GUVs. The inset shows the linear relation between the rate of area increase against time (speed s^{-1}) and irradiation power. The speed is determined by the slope of the linear regions of the curves.

value for the radius r_1 of the adhesion patch of roughly 50%–70% of the original vesicle radius R_0. Due to the particular geometry of adhesion between the deformable spherical vesicle and the rigid flat substrate, such high adhesion patch sizes can

be obtained by unfolding as little as 1%–2% of excess membrane area, a feature clearly seen in the lower section of the curve in Fig. 2a, as sketched by the region (ii). In our strong adhesion conditions, such unfolding corresponds to the complete smearing out of fluctuation modes without significantly stretching the membrane (see discussion in ESI† part). At this stage the prerequisite conditions for measuring photo-induced area increase are completed. However, for the purpose of checking the reliability of the technique, we verify systematically, *i.e.* for each studied GUV, the absence of internal volume loss during the oncoming oxidation step. We thus measure at that stage the adhesion patch radius r_1 and the equator radius R_1 of each adhered GUV to be oxidized (from RICM and fluorescence respectively), and calculate the GUV internal volume V_1 from eqn (1) in ESI.†

Then, as a second step we add erythrosin to the solution, so to reach a final concentration of 25 μM. This step does not perturb the adhered GUVs as evidenced by control experiments described in the ESI† section (see ESI,† Fig. S1). Then constant illumination of the adhered vesicles in the oxidative solution starts, that leads to an increase of the membrane area due to the progressive hydroperoxidation of the lipids, as clearly illustrated by the supporting video and Scheme iii of Fig. 1b. We monitor such increase by measuring under RICM the time evolution of the adhesion patch radius and converting it to the time variation of the relative excess area as plotted in Fig. 2b. The surface area increases with time, eventually reaching a plateau. The kinetics of area increase is solely controlled by the production of oxidized lipid species. Indeed, not only immediate arrest follows if the irradiation is stopped (see ESI,† Fig. S2), but also, as the inset in Fig. 2b shows, is the rate of area production directly proportional to irradiation power.

Once the adhesion patch reaches its stable, maximum value, corresponding to full oxidation, irradiation is stopped and we measure again both adhesion patch radius r_2 and equator radius R_2 in order to calculate the GUV volume V_2. Only if we measure $V_2 = V_1$ within experimental error, the measured increase of membrane area is considered as a reliable result. In fact, above 95% of the evaluated GUVs evolved without any leakage or bursting during oxidation. A full description of this results is given in the ESI† section (Fig. S3) complemented by the discussion of the adhesion patch contrast loss (Fig. S4 and S5, ESI†). The remaining 5% proved that leakage and bursting correspond to events that are right away detectable, since they both deliver results far out of the mean statistics. Thus, the present method appears not only easy to implement but also trustable, a result mainly due to the strong adhesion conditions that create efficiently selective conditions for measuring membrane area increase.

Fig. 3 shows histograms for the plateau values of the relative excess area curves; we find 14.3% and 18.4% for POPC and DOPC, respectively. These values are in very good agreement with results from the micropipette suction method recently published (*i.e.* 15.6% and 19.1% for POPC and DOPC).[8] It is also in good agreement with both recent Single Chain Mean Field theory predictions,[8] and consistent also with molecular simulations from Wong-Ekkabut *et al.*[17]

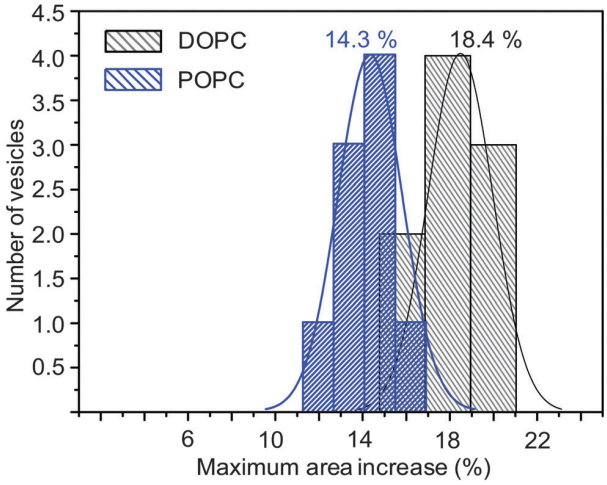

Fig. 3 Histograms built from the maximum relative surface area increase for DOPC and POPC (statistics obtained with 9 vesicles for each lipid type).

Further comparison of our bio-adhesion method with *in situ* oxidation of GUVs under micropipette suction reveals very similar features. There,[8] not only the kinetic curves also reach a plateau, that corresponds to full oxidation of the lipid membrane, but one equally observes a direct relation between rate of area production and irradiation power as well as the immediate arrest of area production when irradiation is stopped. However, this standard technique requires a rather complex micro-manipulation environment and a non-straightforward training for acquiring the appropriated manipulation skills. Besides, the photo-sensitizer aggregation into the micropipette is an issue that may hamper the measure of fully oxidized membrane. Although the drawback of the bio-adhesion method might be the use of biotinylated lipids, one can cite the fluorescent label-free and the RICM real time monitoring as advantages. Indeed, RICM is the only way to simultaneously irradiate the sample and follow the membrane transformations by using the same illumination source.

In summary, GUV adhesion on a bio-adhesive substrate provides a simple and powerful method for extracting molecular area increase of hydroperoxidized lipids. The major features of the method are its simplicity, quantitative nature and capacity to deal with any lipid species that can be self-assembled into a GUV. The method has also potential to quantitatively determine other oxidative processes that eventually lead to vesicle destruction, and can be straightforwardly extended to test the oxidation protection provided by antioxidant species. Although the method is here demonstrated for the particular case of lipid oxidation, it can be applied in many other situations where the area expansion of lipid membranes needs to be monitored, such as osmotic stresses, protein insertion or other oxidation mechanisms. In particular, since the method implies strong adhesion conditions to the membrane, it is particularly useful for processes that do not imply any particular increase of the membrane permeability as could happen from transient pore formation. By contrast, the method will clearly detect any permeation increase, which could be missed by gentler, external force-applying method, as for the electric field method.

Acknowledgements

This work was supported by Centre National de la Recherche Scientifique (CNRS) and is also part of a bilateral agreement USP-Cofecub (no. Uc/Ph 124/11). Pedro H. B. Aoki acknowledges funding from Fundação de Amparo à Pesquisa do Estado de São Paulo (FAPESP 2012/01610-4). C.M. is thankful for support from CNPq under PVE 400997/2014-2.

Notes and references

1 B. N. Ames, M. K. Shigenaga and T. M. Hagen, *Proc. Natl. Acad. Sci. U. S. A.*, 1993, **90**, 7915–7922.
2 E. L. Crockett, *J. Comp. Physiol., B*, 2008, **178**, 795–809.
3 W. Caetano, P. S. Haddad, R. Itri, D. Severino, V. C. Vieira, M. S. Baptista, A. P. Schroder and C. M. Marques, *Langmuir*, 2007, **23**, 1307–1314.
4 H. Sies, *Angew. Chem., Int. Ed. Engl.*, 1986, **25**, 1058–1071.
5 S. P. Stratton and D. C. Liebler, *Biochemistry*, 1997, **36**, 12911–12920.
6 O. Mertins, I. O. L. Bacellar, F. Thalmann, C. M. Marques, M. S. Baptista and R. Itri, *Biophys. J.*, 2014, **106**, 162–171.
7 K. A. Riske, T. P. Sudbrack, N. L. Archilha, A. F. Uchoa, A. P. Schroder, C. M. Marques, M. S. Baptista and R. Itri, *Biophys. J.*, 2009, **97**, 1362–1370.
8 G. Weber, T. Charitat, M. S. Baptista, A. F. Uchoa, C. Pavani, H. C. Junqueira, Y. Guo, V. A. Baulin, R. Itri, C. M. Marques and A. P. Schroder, *Soft Matter*, 2014, **10**, 4241–4247.
9 R. Dimova, K. A. Riske, S. Aranda, N. Bezlyepkina, R. L. Knorr and R. Lipowsky, *Soft Matter*, 2007, **3**, 817–827.
10 R. Lehner, J. Koota, G. Maret and T. Gisler, *Phys. Rev. Lett.*, 2006, 96.
11 M. L. Hisette, P. Haddad, T. Gisler, C. M. Marques and A. P. Schroder, *Soft Matter*, 2008, **4**, 828–832.
12 J. Radler and E. Sackmann, *J. Phys. II*, 1993, **3**, 727–748.
13 D. S. Pellosi, B. M. Estevao, J. Semensato, D. Severino, M. S. Baptista, M. J. Politi, N. Hioka and W. Caetano, *J. Photochem. Photobiol., A*, 2012, **247**, 8–15.
14 A. Albersdorfer, T. Feder and E. Sackmann, *Biophys. J.*, 1997, **73**, 245–257.
15 R. Bruinsma and E. Sackmann, *C. R. Acad. Sci., Ser. IV: Phys., Astrophys.*, 2001, **2**, 803–815.
16 D. Cuvelier and P. Nassoy, *Phys. Rev. Lett.*, 2004, 93.
17 J. Wong-Ekkabut, Z. Xu, W. Triampo, I. M. Tang, D. P. Tieleman and L. Monticelli, *Biophys. J.*, 2007, **93**, 4225–4236.

Supporting Information

Bioadhesive giant vesicles for monitoring hydroperoxidation in lipid membranes

P. H. B. Aoki[1,2,3], A. P. Schroder[1], C. J. L. Constantino[2] and C. M. Marques[1]

[1]Institut Charles Sadron, Université de Strasbourg,
CNRS UP 22, F-67034 Strasbourg Cedex 2, France.

[2] Faculdade de Ciências e Tecnologia, UNESP Universidade Estadual Paulista,
Presidente Prudente, SP, 19060-900, Brazil

[3]São Carlos Institute of Physics, University of São Paulo,
CP 369, 13560-970 São Carlos, SP, Brazil

Materials

All phospholipids were purchased from Avanti Polar Lipids: 1-palmitoyl-2-oleoyl-sn-glycero-3-phosphocholine (POPC), 2-dioleoyl-sn-glycero-3-phosphocholine (DOPC), 1,2-distearoyl-sn-glycero-3-phosphoethanolamine-N-[biotinyl(polyethyleneglycol)-2000] (DSPE-PEG(2000)-Biotin) and 1,2-dipalmitoyl-sn-glycero-3-phosphoethanolamine-N-(7-nitro-2-1,3-benzoxadiazol-4-yl) (NBD). Xanthene erythrosin B, 3-aminopropyltriethoxysilane (APTES), streptavidin and neutrAvidin®-tetramethylrhodamine conjugate were purchased from Sigma-Aldrich. Glutaraldehyde (8%) was purchased from Polysciences. All chemicals were used without further purification

Streptavidin-coated substrates

Glass coverslips (30 mm in diameter) were: (i) cleaned with a piranha solution (75% of H_2SO_4 and 25% of H_2O_2), (ii) rinsed with milli-Q water, (iii) amino-functionalized by immersion in ethanol solution of 2% APTES for 5 minutes, (iv) heated at 110 ^oC in the oven for 15 minutes in order to stabilize the amino-silane layer, (v) incubated in a 4% glutaraldehyde solution for 1 hour and subsequently rinsed with milli-Q water, (vi) incubated for one hour in a saline phosphate buffer (PBS) solution containing 0.05 mg/mL of streptavidin and (vii) rinsed with PBS solution. This protocol was already described in[1-2]. For the purpose of evaluating the reliability of the above protocol, we initially imaged, using fluorescence microscopy, a streptavidin layer obtained by first mixing streptavidin and rhodamine modified neutravidin (ratio 1:1), prior to further incubation keeping the same procedure as above.

Buffer solutions and biotinylated GUVs electroformation.

GUVs were prepared by the electroformation[3] method. Biotinylated DOPC and POPC GUVs were prepared by adding 2 mol % of DSPE-PEG(2000)-Biotin. Fluorescent GUVs were obtained by adding 0.5 mol % of NBD. Briefly, 10 μL of a chloroform solution containing the lipid mixture (1 mg/ml) were spread on the surfaces of two conductive ITO (Indium Tin Oxide) glasses, which were then assembled with their conductive sides facing each other and separated by a 2-mm-thick Teflon frame, so to form a growing chamber. After drying under vacuum, the electroswelling chamber was filled with 200 mOsm kg^{-1} sucrose solution and connected to an alternating power generator at 1 V with a 10 Hz frequency for 2 h. Vesicles were then diluted 6 times in a 200 mOsm kg^{-1} PBS solution and dropped onto the streptavidin coated surfaces. The osmolarities of the sucrose and PBS solutions were measured with a cryoscopic osmometer Osmomat 030 (Gonotec, Berlin, Germany) and carefully matched to avoid osmotic pressure effects. The interplay between sucrose and PBS osmotically matches the inner and outer compartments of the vesicles and avoids their swelling and deswelling, especially under the strong adhesion conditions of the present study. An erythrosin-containing (1 mOsm kg^{-1}) PBS solution was also prepared, with an osmotic pressure also adjusted to 200 mOsm kg^{-1}.

Observation and irradiation under an optical microscope

Confocal microscopy images were taken for the purpose of illustration of the GUV adhesion (see Fig 1a in the paper); we used a TE2000 (Nikon, Japan) inverted microscope, equipped with a 100X oil-immersion objective, and a C1 confocal scanning head. Most of the present work, in particular GUV oxidation under irradiation and subsequent RICM observation of GUV adhesion, was performed under a TE200 inverted microscope (Nikon, Japan), equipped with a 100X oil immersion, a 40X DIC or a 40X phase contrast objectives. Images were acquired with a Diagnostic Instruments IN1800 digital camera and analyzed using a homemade software. Transmission (mainly DIC or phase contrast), fluorescence, and reflection interference contrast microscopy (RICM)[4] were used to image the GUVs. RICM allows to observe the GUV membrane in the vicinity of the substrate,[4] enabling in particular to follow the kinetics of adhesion of the biotinilated GUVs on the streptavidinated substrate (see Figure 1 and 2 in the paper). The RICM observation mode requires the association of a certain number of optical elements, i.e. a narrow band filtered illumination, a polarizer, an oil objective equipped with an outer quarter wave plate adapted to the observation wavelength, and an analyzer. In this study, we imaged the GUV adhesion using two illumination wavelengths, obtained using two narrow-band filters (Melles-Griot, bandwidth 10 nm): 436 nm (‘blue’) or 547 nm (‘green’). The blue filter enabled RICM observation without vesicle perturbation, since erythrosin absorption around 436 nm is very small,[5] while the green filter was used for simultaneous RICM observation and photoactivation of erythrosin. In both wavelengths good enough interference images were obtained, enabling a precise measurement of the GUV adhesion patch dimensions, even though the quarter wave plate of our 100X objective was adapted for the green wavelength. The total

density power in the RICM mode at 547 nm, i.e. during oxidation, was ca. 10 W/cm^2, as measured previously.[6]

Surface area increase

We consider a spherical vesicle with apparent radius R_0, i.e. of volume $V_0 = \frac{4}{3}\pi R_0^3$. Its apparent area S_0 is related to R_0 by $S_0 = 4\pi R_0^2$ We suppose that the vesicle is of real area $S_{real}>S_0$ (some of the area is hidden in sub-optical thermal fluctuations). Let the vesicle adhere to a substrate, with preserved volume, so that its adhesion patch is round shaped with radius r, and the upper, non-adhered part is a spherical section of radius R. Then the volume V_0 and the apparent surface S ($S_0<S<=S_{real}$) of the adhered vesicle can be expressed as a function of R and r.

$$V_0 = \frac{2}{3}\pi R^3\left(1+\frac{3}{2}\left(1-\frac{r^2}{R^2}\right)^{\frac{1}{2}}-\frac{1}{2}\left(1-\frac{r^2}{R^2}\right)^{\frac{3}{2}}\right) \quad (1)$$

$$S = \pi r^2 + 2\pi R^2\left(\left(1-\frac{r^2}{R^2}\right)^{\frac{1}{2}}+1\right) \quad (2)$$

Expressing now all lengths in units of R_0, the radius R of a vesicle adhering under constant volume can be expressed as

$$R = \frac{1}{16}\left(\frac{r^8}{\Delta}+r^4+\Delta\right) \quad (3)$$

with Δ given by:

$$\Delta = \left(r^{12}+128r^6+16\left(\left(\left(r^6+16\right)\left(r^6+32\right)^2\right)^{\frac{1}{2}}+128\right)\right)^{\frac{1}{3}} \quad (4)$$

Erythrosin addition effect

A stock solution of erythrosin was prepared, at 1 mOsm kg^{-1} concentration into a 200 mOsm kg^{-1} PBS buffer. A small volume, typically less than five microliters of this solution, was added at the end of stage ii (Figure 1.b) into the observation chamber containing the adhered biotinilated GUVs, so to reach the final concentration 25 µM of erythrosin. We checked that this addition of erythrosin did not induce any modification of the GUV adhesion state. This was done following the evolution of the adhesion patch radius over minutes, in absence of 'green' irradiation. Figure S1 shows such typical evolution of (r); only when the 'green' irradiation starts (P=10 W/cm^2, λ=547 nm) the adhesion patch undergoes an immediate and rapid increase, due to membrane area increase.

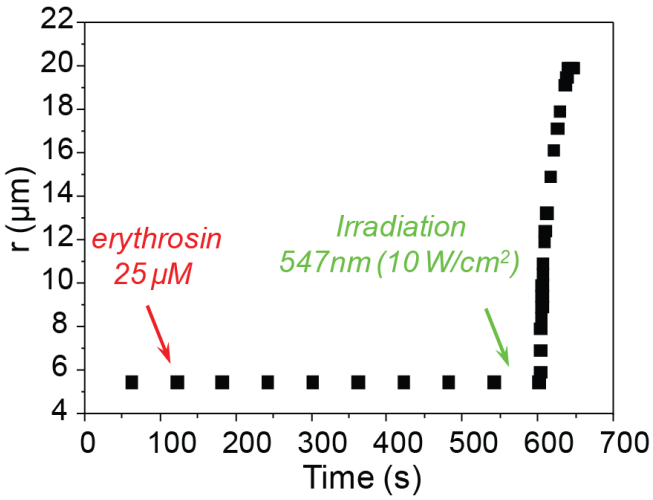

Figure S1: evolution of the adhesion patch radius (r) of a biotinilated GUV after the addition of erythrosin in the surrounding medium (time of addition is shown by the red arrow). No effect is detected for minutes; only when 'green' irradiation starts (green arrow) the radius is seen to increase abruptly, corresponding to the membrane specific area increase, resulting from the hydroperoxidation of the lipid chain double bonds.

Start-stop experiments

We performed start-stop experiments, submitting adhered biotinilated DOPC or POPC GUVs dispersed in an erythrosin-containing buffer (25 μM of erythrosin) to successive 'on-off' irradiation stages, in order to see how membrane area increase correlates with light-induced oxidation. In practice, considering an adhered, stable GUV as that sketched on state (ii) in Figure 1.b, we first measure its internal volume from both the radius (r) of its adhesion patch and from its equator radius (R), using low power, 'blue', 435 nm light. Then, focusing on the substrate plane so to get an interference RICM image of the adhesion patch, we submit the GUV to successive 'on-off' irradiation steps, under continuous imaging, corresponding to successive switching from 'blue' light to 'green', 547 nm, high power irradiation. The membrane adhesion patch can be continuously imaged, provided that the camera gain and/or exposure time are manually changed with irradiation wavelength, which takes less than one second. The evolution with time of the relative surface area increase is given in Figure S2 for a typical experiment. It can be seen that there is no delayed effect when starting or stopping the irradiation. When the surface area reaches its maximum value, the GUV is imaged in blue and its volume is again measured so to check if the whole process was achieved at constant volume. This test proves the correlation existing between sensitizer excitation and membrane lipid double bond(s) hydroperoxydation.

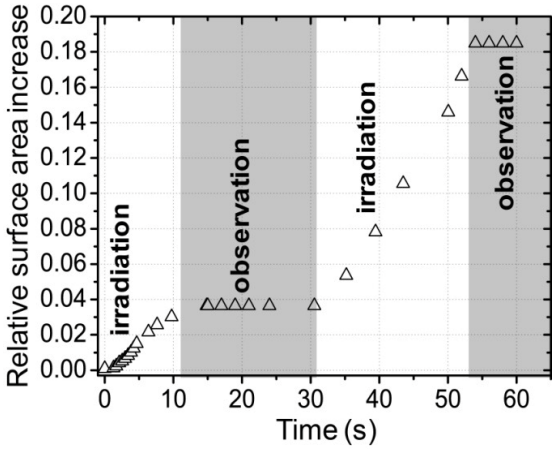

Figure S2: relative surface area increase as a function of time, alternating irradiation ('green', full power) and observation ('blue'), for an adhered biotinylated DOPC GUV into a buffer solution containing 25 μM of erythrosin.

Leakage

It was crucial to verify that the membrane area increase with oxidation, that is revealed by the increase of the GUV adhesion patch size, is a process that takes places without any leakage of the vesicle internal solution. For that purpose the following protocol has been applied for each studied GUV: at the end of the first adhesion stage (sketched by ii in Figure 1.b), we systematically measured both the adhesion patch radius r_1 and the equator radius R_1 (from RICM and fluorescence respectively), that allowed us to calculate the GUV internal volume (V_1). The erythrosin was then added into the solution, and after circa. one minute the irradiation was started ('green', high power illumination) while continuous image acquisition was performed. Once the adhesion patch reached a new, stable value, the irradiation was stopped and the adhesion patch and equator radii r_2 and R_2 were measured, and the internal volume (V_2) calculated. Only if V_1 and V_2 were identical within the experimental error the GUV was validated and its increase in membrane area calculated. Figure S3 presents the V_2/V_1 values for all DOPC and POPC selected vesicles; one gets V_2/V_1 =1.00 with less than 2% error. Only very few GUVs experienced bursting or leakage during oxidation (less than 5%). There is little to say about GUV bursting: this may be due to any membrane default and is of low interest here. Bursted GUVs are obviously not taken into account. Concerning the GUVs that undergo leakage ($V_2/V_1<1$) with oxidation, the fact that they represent a small fraction of the whole (<5% only) is certainly due to some specific property of oxidized DOPC and POPC. The bilayer internal cohesion force remains strong enough, i.e. higher than the tension generated by the biotin-streptavidine adhesion energy. The important point here is that these vesicles show a relatively high level of leakage (when they do leak), typically $V_2/V_1<0.5$. This is certainly due to the high tension of the bilayer imposed by the present adhesion conditions; indeed the biotin-streptavidin bond has one of the highest binding energy in the bio-world. Thus, the leakage appears clearly

from the measure of the adhesion patch radius. There is in fact no need to check the final GUV volume V_2; following simply the adhesion radius evolution with time is enough to guess that the GUV underwent leakage.

Finally, the fact that DOPC and POPC GUVs rarely leak during oxidation leads us to the believe that the initial, non oxidized GUVs that are left to sediment and adhere on the streptavidinated bottom surface, reaching stage (ii) on Figure 1.b, should identically reach this stable, stretched state with smeared thermal fluctuations without having sustained any leakage.

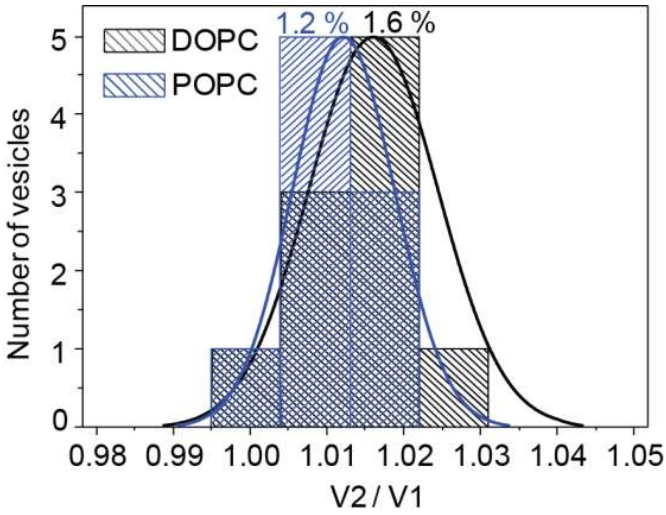

Figure S3: distribution of the V_2/V_1 values for all DOPC and POPC studied GUVs. V_1 is the volume before and V_2 after oxidation. V_1 and V_2 are calculated from r and R, using the formula of the volume of a truncated sphere.

Loss of contrast

The contrast in the RICM image of a stable, oxidized membrane appears lower than the contrast of the initial patch, i.e. before oxidation started, as shown in Figure 1. In fact, the lowering of the contrast was seen to start at various moments of the oxidation process, depending on the vesicle, but always after several tens of seconds of irradiation. Two examples are given in the following Figure S4; it can be seen that the loss of contrast may follow the stabilization of the area increase (left), or start before it (right). However, in both situations depicted by Figure S4, the area increase remains unmodified by the gray level variation: in the case of a membrane area still on its increasing stage when the contrast starts to decrease, no modification of the area rate of increase is observed (right); if the area already reached its stable final value before the gray level starts to decrease, no modification of the area is observed (left). Again, membrane area is here calculated from geometrical values of r (i.e. in real time from RICM) but with a systematic measure of the equator radius R at the end of the process, in order to control that the internal volume of the GUV remained constant through the overall process (see above). We argue that it's not reasonable to invoke some leakage (with sucrose/glucose exchange) while the adhered membrane keeps its internal volume. Any pore opening followed by leakage is not compatible with volume conservation, since the membrane is under some strong tension due to the adhesion. Understanding this gray level decrease is also beyond the scope of this article, but we can invoke at least three mechanisms: i) an increase of the membrane-substrate distance, due to strong modification of the membrane-substrate interactions (we should remind that an important fraction of the membrane surface should be populated with - OOH groups at the end of the hydroperoxidation process); ii) the lateral membrane area increase of 15-19% might also contribute to a change in the membrane substrate distance in the patch region, because of some

geometrical hindrance that reduces lateral diffusion of lipids out of the adhesion patch, due to the high concentration of biotin-streptavidin links; and iii) the membrane should also be thinner by a factor of circa 8% since its surface area increases by 14-19%. Other reasons might also be at the origin of that loss of contrast, but our experiments clearly show no leakage, as demonstrated by Figure S3.

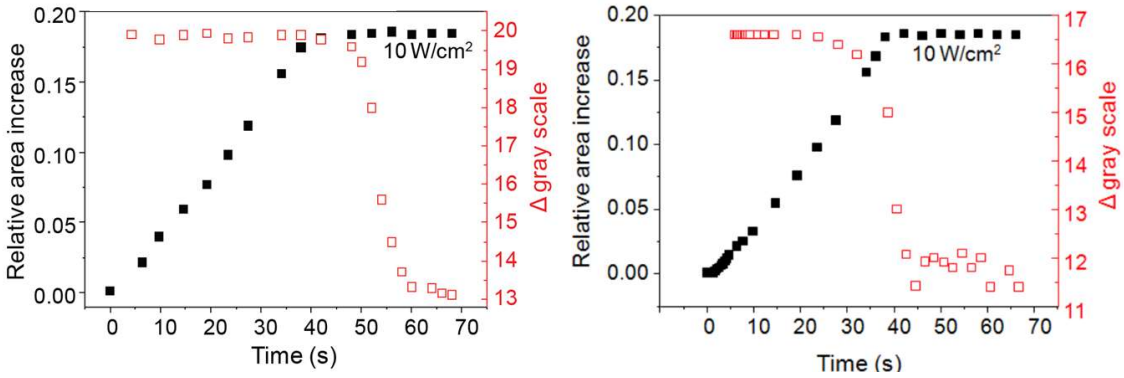

Figure S4: time evolution of membrane area (as measured from r, the adhesion patch radius) and contrast between the inside and outside of the adhesion patch, for two DOPC vesicles. For each vesicle we measure V_2 from r_2 and R_2, and check that V_2=V_1 within the experimental error (see Figure S3).

Finally, for a matter of illustration, Figure S5 shows a typical evolution of the adhesion patch under continuous irradiation. Figures S5a and S5b correspond to the starting point and the ending point of area increase, respectively. Only 90 seconds later, while illumination still goes on, one can observe the dramatic effect of the membrane rupture that is highlighted by the presence of some inhomogeneous membrane repartition on the substrate. Besides, one could wonder why on Figure S5c the original adhesion patch (the one created prior to oxidation process) is preserved, while the part of the patch that was generated during oxidation appears strongly modified after the membrane rupture. One can deduce from these observations that not only the mechanism of oxidation is complex, modifying strongly both the membrane properties and the interactions of the membrane with our streptavidinated substrate, but also the adhesion geometry used to reveal

lipid area increase is itself complex, with a finite number of ligands on the membrane, a finite diffusion coefficient of these ligands, amongst others, all these factors contributing possibly to the observed inhomogeneities and contrast variations as seen in RICM. However, we undoubtedly were able to reveal and measure the lipid area increase due to oxidation, from the round-shaped adhesion patches measured at stages II and III, which correspond to stable states.

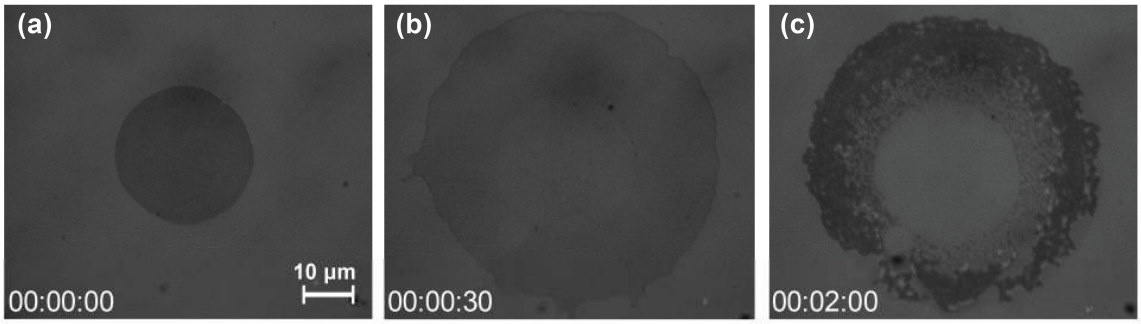

Figure S5: RICM evolution of the adhesion patch (a) before, (b) after irradiation and (c) after vesicle collapse.

Strong adhesion, membrane tension, GUV shape

We calculate the volume of our adhered GUVs assuming that their shape is that of a truncated sphere. Checking this point with confocal microscopy is easy but the same information can be obtained using other arguments, as obtained from the literature. For that we need first to evaluate the membrane tension of the adhered GUVs. For that we refer to the seminal paper of E. Evans,[7] that relates the contact angle, the tension and the adhesion energy between the membrane and the substrate, comparing the limit situation defined by a high density of linkers to the case of a low density of linkers. In the present study, we argue that we are close to the limit defined as that of a 'high density of linkers'. Indeed, the vesicles adhere on a glass that is functionalized with a monolayer of streptavidin molecules, the area of which is circa 25 nm^2. The biotin molar fraction in the membrane is 2%, corresponding to an area concentration of circa one biotin per 33 nm^2 (considering a lipid area of 65 $Å^2$). Thus, the area concentrations of ligands and receptors match approximately, a condition that we imposed so to optimize the adhesion force and efficiency. According to,[7] of importance for the calculation of the membrane tension is the ratio lg/lb, of the distance between two neighboring links in the adhesion patch, to the characteristic distance of the adhesion interaction. Here lg is of the order of 5 nm, while lb is of the order of 10 nm (i.e. a fraction of the PEO contour length, the carbon spacer that links the biotin head to the lipid head); lg/lb is therefore of the order of, or even smaller than one. In this case, according to,[7] the Youngs equation $T=W(1-\cos\theta)$ is valid and enables to calculate the membrane tension knowing W, the adhesion energy, and θ, the membrane-substrate contact angle. First, W can be calculated easily: W=w.f, and f is the surface area concentration of links in the adhesion patch, and w=40 k_BT is the typical binding energy of a biotin-streptavidin bond; thus W=5 mN/m considering one link per 30 nm^2. Furthermore, from our RICM images one can determine that θ is always higher than

60°, since no interference ring is visible around the adhesion patch. This leads to a value for the membrane tension of circa T=2.5 mN/m (taking θ=60°). This value is an overestimation since we consider that almost 100% of the streptavidins covering the substrate are linked to a biotin of the membrane in the adhesion patch region. However, even for a five times smaller value, could we still consider that the membrane tension is high enough so to smear out the membrane thermal fluctuations. Indeed, experimental studies of GUV deformation under suction, using a micropipette device, have clearly shown that for tensions higher than 0.5-1.0 mN/m membrane thermal fluctuations can be considered as smeared out, see for example.[8] So we argue that in our adhesion conditions, our vesicles can indeed be considered as being tensed enough so that no significant thermal fluctuations remain. Any measured increase of membrane surface area is therefore a real increase of the specific membrane area, and not a simple smearing out of some non visible, excess of membrane that would be stored under the form of thermal fluctuations.

A second argument is now necessary to establish that the shape of our adhered GUVs is that of a truncated sphere. It is known that the bending energy of the membrane fights against the establishment of the contact angle in the vicinity of the substrate surface. For papers treating this situation, one can cite.[9] The effect of a finite bending modulus is that, out of the adhesion patch, the membrane becomes a spherical cap only after a distance λ from the patch border, with $\lambda=(\kappa/\sigma)^{1/2}$, κ is the bending rigidity and σ is the membrane tension. Taking $\kappa=20\ k_BT$ and $\sigma=0.2$ mN/m reads $\lambda=20$ nm, a very small distance compared to the overall dimension of the GUV. Therefore, the deviation from the pure truncated sphere can be ignored in the present case.

References

1. R. Lehner, J. Koota, G. Maret and T. Gisler, *Physical Review Letters*, 2006, **96**.
2. Y. T. L. Sun, N. K. Mani, D. Baigl, T. Gisler, A. P. Schroder and C. M. Marques, *Soft Matter*, 2011, **7**, 5578-5584.
3. M. I. Angelova and D. S. Dimitrov, *Faraday Discussions*, 1986, **81**, 303-311.
4. J. Radler and E. Sackmann, *Journal De Physique Ii*, 1993, **3**, 727-748.
5. D. S. Pellosi, B. M. Estevao, J. Semensato, D. Severino, M. S. Baptista, M. J. Politi, N. Hioka and W. Caetano, *Journal of Photochemistry and Photobiology a-Chemistry*, 2012, **247**, 8-15.
6. W. Caetano, P. S. Haddad, R. Itri, D. Severino, V. C. Vieira, M. S. Baptista, A. P. Schroder and C. M. Marques, *Langmuir*, 2007, **23**, 1307-1314.
7. E. A. Evans, *Biophysical Journal*, 1985, **48**, 185-192.
8. E. Evans and W. Rawicz, *Physical Review Letters*, 1990, **64**, 2094-2097.
9. U. Seifert and R. Lipowsky, *Physical Review A*, 1990, **42**, 4768-4771.